Hurricane-forced upwelling and chlorophyll *a* enhancement within cold-core cyclones in the Gulf of Mexico

Nan D. Walker

Department of Oceanography and Coastal Sciences/Coastal Studies Institute Earth Scan Laboratory, Louisiana State University, Baton Rouge, Louisiana, USA

Robert R. Leben

Colorado Center for Astrodynamics Research, University of Colorado, Boulder, Colorado, USA

Shreekanth Balasubramanian

Coastal Studies Institute Earth Scan Laboratory, Louisiana State University, Baton Rouge, Louisiana, USA

Received 8 June 2005; revised 22 August 2005; accepted 24 August 2005; published 30 September 2005.

[1] Clear skies, subsequent to Hurricane Ivan's passage across the Gulf of Mexico in September 2004, provided a unique opportunity to investigate upper ocean responses to a major hurricane. Oceanic cyclonic circulation was rapidly intensified by the hurricane's wind field (59–62 m s^{-1}), maximizing upwelling and surface cooling (3–7°C) in two large areas along Ivan's track. Upward isothermal displacements of 50–65 m, computed from wind stress and sea surface height changes, caused rapid ventilation of thermoclines and nutriclines, leading to phytoplankton blooms with peak concentrations 3–4 days later. Wind speed changes along Ivan's track demonstrated that the cool waters (20–26°C) provided immediate negative feedback to the hurricane's intensity. Although our study focused on a relatively small ocean area, it revealed that mesoscale cyclones, in addition to warm anticyclones, may play an important role in producing along-track hurricane intensity changes. **Citation:** Walker, N. D., R. R. Leben, and S. Balasubramanian (2005), Hurricane-forced upwelling and chlorophyll *a* enhancement within cold-core cyclones in the Gulf of Mexico, *Geophys. Res. Lett.*, *32*, L18610, doi:10.1029/2005GL023716.

1. Introduction

[2] Hurricane Ivan was a classic hurricane that formed over the tropical Atlantic Ocean on 2 Sep 2004. Upon entering the southern Gulf of Mexico (GoM) as a category 4 hurricane on 14 Sep, it moved NNW towards New Orleans, LA, at 5.4 m s^{-1} with a maximum wind speed of 62 m s^{-1} (Figure 1). On 15 Sep, it altered course (as predicted) to the NNE, making landfall ten hours later near Gulf Shores, AL as a strong category 3 hurricane [*National Hurricane Center* (*NHC*), 2004].

[3] Sea surface temperature (SST) above 26°C is essential for hurricane development and maintenance [*Buyers*, 1974]. Previous research has shown that GoM warm core rings (WCRs) can rapidly increase hurricane intensity due to the fluxes of latent and sensible heat from the warm (>28°C) and deep (>150 m) mixed layer [*Shay et al.*, 2000]. In contrast, negative oceanic feedback and hurricane weakening has been documented over waters below 26°C [*Monaldo et al.*, 1997]. Hurricane-forced sea surface cooling results mainly from vertical mixing and entrainment, transient upwelling, and evaporative heat loss to the atmosphere [*Price*, 1981; *Sanford et al.*, 1987]. Previous observational and modeling studies have shown that an asymmetrical SST response to hurricane wind forcing is typical, with greatest cooling east of the hurricane's track. There, winds are strongest and the wind stress vector turns clockwise through time, maximizing surface divergence and upwelling [*Price*, 1981; *Stramma et al.*, 1986; *Monaldo et al.*, 1997]. Although hurricane-forced cooling can affect future storms that pass over the same area [*Brand*, 1971] and even the parent storm [*Black and Holland*, 1995], real-time SST information is not easily incorporated into hurricane intensity prediction models. This lack of crucial information is a contributing factor to the poor reliability in forecasting hurricane intensity changes [*Emanuel*, 1999].

[4] Clear skies, subsequent to Ivan's passage across the GoM, provided a unique opportunity to study physical and biological changes of the upper ocean using satellite data from both passive and active sensors. Integration of sea surface height (SSH) data with satellite-derived SSTs and chlorophyll *a* (Chla) enabled a comparison of ocean responses within cold-core cyclones and WCRs (anticyclones). Our analysis revealed sea surface cooling of 3–7°C and elevated Chla concentrations over two large areas of pre-existing cyclonic circulation along Ivan's track. Ivan's wind speeds decreased twice over the GoM [*NHC*, 2004], despite crossing the LC and a large WCR. Both intensity changes occurred subsequent to the evolution of 20–26°C SSTs along its track, suggesting rapid negative oceanic feedback from two cyclones.

2. Satellite Data

[5] SST was quantified using GOES-12 night-time composite images. A major advantage of GOES data is frequent repeat coverage (48 images/day) which enables removal of cloud cover, improving feature detection and SST accuracy [*Legeckis et al.*, 1999; *Walker et al.*, 2003]. Chla concentrations were computed from SeaWiFS data using the NASA OC2 algorithm [*O'Reilly et al.*, 1998]. Altimeter data from Jason-1, TOPEX/POSEIDON,

0094-8276/05/2005GL023716$05.00

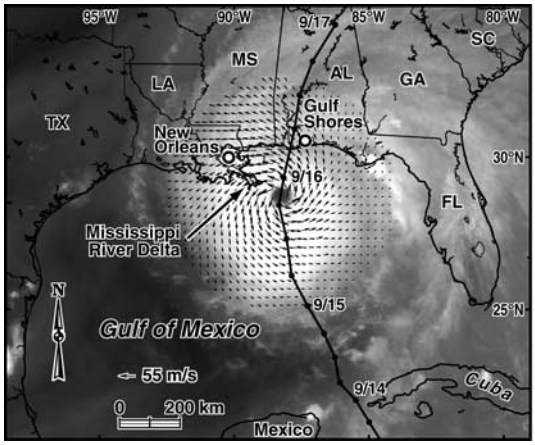

Figure 1. GOES-12 water vapor image on 15 Sep (2245 UT) showing Ivan, the GoM, and other pertinent locations. Ivan's 6-hour positions are depicted with black dots. NHC vector winds are superimposed (http://www.aoml.noaa.gov/).

and Geosat Follow-on were used to compute SSH using techniques described by *Leben et al.* [2002].

3. Upper Ocean Cooling and Relationship to Cyclones

[6] The GOES SST composite of 17 Sep revealed two large regions of cooling proximate to Ivan's track, where SSTs of 20–26°C were detected over 38,900 km^2 (Figure 2b). SSTs prior to the event (9 Sep) were 28–30°C (Figure 2a; Table 1). SST change averaged −3.8°C in the northern feature and −4.1°C in the southern feature, with respective maxima of −5.9° and −7.4°C (Table 1). Mean SST change of −1.9°C occurred within the WCR, which separated the areas of maximum cooling (Figures 2a and 2b; Table 1).

[7] SSH data showed pre-existing cyclonic circulation in the areas where the extreme cooling occurred (Figures 2a and 2b). The hurricane wind field (33–62 m s^{-1}) intensified cyclonic circulation in both areas, as SSH changes of −5 to −20 cm were detected between 9 and 17 Sep (Figures 2a–2c). North of the WCR, maximum cooling (SST change > −5°C) occurred 40 to 90 km east of Ivan's track in an area of maximum SSH change (Figure 2c). Its location agreed with results of *Price* [1981], who found that maximum cooling for rapidly moving hurricanes usually occurs 30–150 km to the right of the track. MODIS SST data (not shown) revealed a frontal eddy cyclone in this location before hurricane passage. South of the WCR, maximum cooling occurred within the area of cyclonic circulation, closest to Ivan's track (Figure 2b). The region of extreme cooling (SST change > −5°C) extended 20 km east of and 80 km west of Ivan's track. It extended further west than would be expected based on previous research. Some westward advection of upwelled waters may have occurred between Ivan's passage and image acquisition, as strong currents (~60 cm s^{-1}) occurred along the outer margin of the WCR on 17 Sep (Figure 3c). Extreme cooling was not observed further east as this was an area of positive SSH, connecting the WCR with the LC. Although cool wakes of 1–6°C have been detected after hurricane passage in several ocean areas [*Price*, 1981; *Stramma et al.*, 1986; *Monaldo et al.*, 1997], our results demonstrate maximum cooling in regions of cyclonic circulation along Ivan's track.

[8] Surface wind data, available every 6 hours from the National Hurricane Center [*NHC*, 2004], revealed that Ivan's winds decreased twice during its transit of the GoM (Figure 2c). The first intensity change (from 62 to 59 m s^{-1}) was observed on 15 Sep 1200 UTC, soon after evolution of 20–26°C water in the southern upwelling

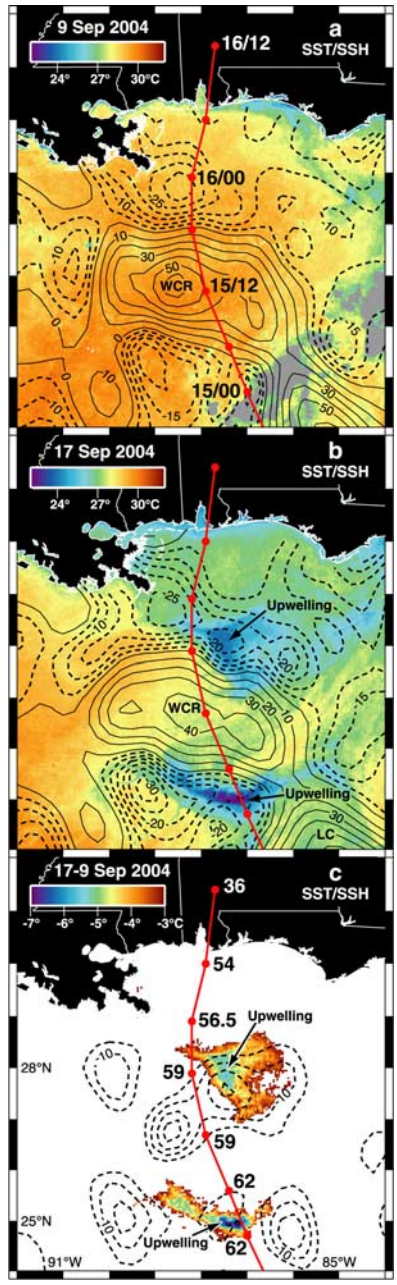

Figure 2. GOES SSTs (°C) with SSH 5 cm contours superimposed on (a) 9 Sep and (b) 17 Sep. Negative SSH indicates cyclonic circulation. (c) SST and SSH differences (17–9 Sep). Winds speeds at 10m (m s^{-1}) are shown along Ivan's track. Ivan's 6-hour positions are shown in a-c. Clouds are gray.

Table 1. SST (°C) for the Northern (UN) and Southern (US) Upwelling Regions, and WCR: September 2004

Region	9	17	19	ΔX Mean 17-9	ΔX Max 17-9
UN[a] (25,000 km^2)	29.2	25.4	27.1	−3.8	−5.9
US[a] (14,000 km^2)	28.9	24.8	26.4	−4.1	−7.4
WCR (19,000 km^2)	29.4	27.5	28.3	−1.9	−3.6

[a]Statistics are for areas where SST change exceeded 3°C.

region. The second change (from 59 to 56.5 m s^{-1}) occurred between 15 Sep 1800 and 16 Sep 0000 UTC (Figures 2a and 2c), in close proximity to the northern upwelling feature. We conclude that the two large areas of cool water (<26°C over 38,000 km^2) provided rapid negative feedback to Hurricane Ivan.

3.1. Cyclone Intensification and Upward Displacement of the Thermocline

[9] GoM cyclones are regions of vigorous sub-surface upwelling and upward doming of cool water where the top of the thermocline is typically 50–60 m below the sea surface [*Biggs and Muller-Karger*, 1994; *Zimmerman and Biggs*, 1999; *Gilligan and Blaha*, 2003]. The isopycnal displacement of the thermocline due to storm-induced upwelling can be computed as $\eta = \tau/\rho\ f\ U_h$; where τ is wind stress, ρ is water density, f is the Coriolis force, and U_h is hurricane transit speed [*Price et al.*, 1994; *Babin et al.*, 2004]. Based on maximum wind speeds of 59–62 ms^{-1}, τ values of 18.7–21.9, and a transit speed of 5.4 m s^{-1} we estimated that the thermocline upwelled from depths of 53 to 62 m within the areas of maximum SST change. Using SSH data, we also computed isotherm upwelling ($\Delta\eta$) from the change in SSH anomaly (Δh) using the reduced gravity approximation $\Delta\eta = -g/g'\ \Delta h$ [*Shay et al.*, 2000]. Assuming a g' value of 0.03 ms^{-2} that is representative of gulf-wide conditions we estimate upward displacement of an isotherm of 32.7 m for every −10 cm change in SSH. The observed −15 to −20 cm changes in SSH yielded isotherm displacements of 50–65 m, which are consistent with our estimates based on wind stress.

3.2. Chlorophyll *a* Changes Within Cyclones and Eddy Entrainment

[10] Time-sequence SeaWiFS imagery revealed large-scale enhancement of Chla concentrations within the two large upwelling regions (Figures 3a–3c). Peak concentrations occurred on 19 Sep (Figure 3c) (Table 2) when mean values above 1 mg m^{-3} covered 9000 km^2 and 6200 km^2 (in northern and southern features, respectively). Temporal Chla changes were assessed by including larger areas than those defined by 1 mg m^{-3}, as the features were not stationary after generation. Within the northern area of cooling, concentrations increased from 0.36 mg m^{-3} (before Ivan) to 0.81 mg m^{-3} (on 19 Sep) over 27,000 km^2 (Table 2). In the southern region, mean concentrations increased from 0.24 mg m^{-3} to 0.99 mg m^{-3} over 13,000 km^2 (Table 2). Peak concentrations lagged Ivan's passage by 3 and 4 days in the northern and southern features, respectively. The predicted 50–65 m upward isotherm displacement would have injected high concentrations of nitrate into surface waters, since nitraclines within GoM cyclone centers are typically found near 50–70 m [*Biggs and Muller-Karger*, 1994; *Zimmerman and Biggs*, 1999].

[11] Hurricane-induced Chla enhancement can result from upward entrainment of phytoplankton to the surface from the deep Chla maximum or from new production [*Babin et al.*, 2004]. Our results indicate that both processes contributed to the enhancement in surface Chla. In the northern feature, mean Chla values increased from 0.36 mg m^{-3} on 8 Sep to 0.50 mg m^{-3} on 17 Sep, 1.5 days after Ivan's passage (Table 2). However, peak mean

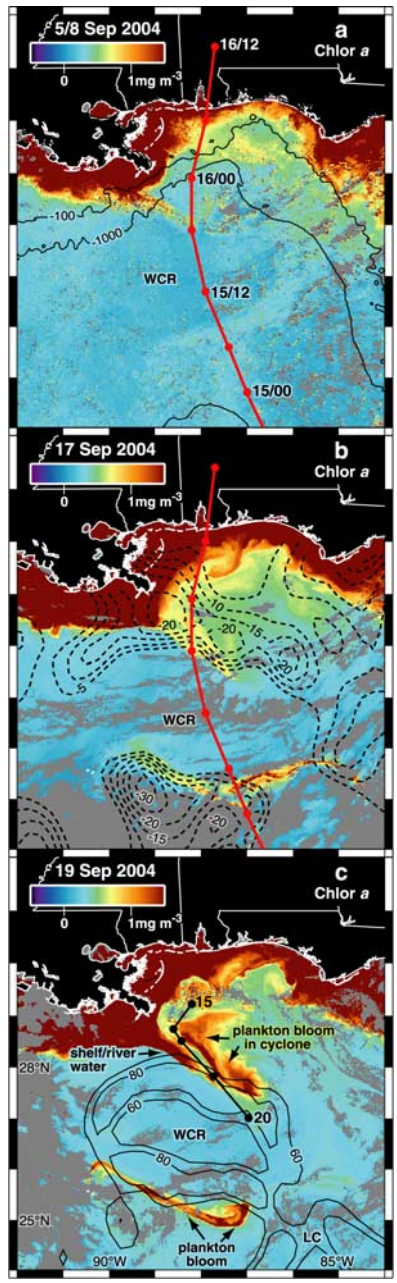

Figure 3. Chla (mg m^{-3}) computed from mean values on (a) 4 days (3, 5, 7, 8 Sep); (b) 17 Sep; and (c) 19 Sep. In (a) and (b), Ivan's 6-hour positions are shown. In (b), negative SSH data for 17 Sep are shown. In (c), SSH-derived 60 and 80 cm s^{-1} speed isotachs for 17 Sep are superimposed. NDBC buoy positions, obtained at irregular intervals, from 15 to 20 Sep are also shown. Clouds are gray.

Table 2. Chla Changes (mg m^{-3}) for Northern (UN) and Southern Upwelling (US) Regions: September 2004

					ΔX Mean		
Region	3/8[a]	17	19	27/29[b]	17-8	19-17	19-8
UN (27,000 km^2)	0.36	0.50	0.81	0.45	+0.14	+0.31	+0.45
US (13,000 km^2)	0.24	0.46	0.99	0.24	+0.22	+0.53	+0.75

[a]Mean value for 3, 5, 7, and 8 September.
[b]Mean value for 27 and 29 September.

concentrations of 0.81 mg m^{-3} occurred a full 2 days later (Figures 3b and 3c). In the southern feature, mean Chla values increased from 0.24 mg m^{-3} to 0.46 mg m^{-3} between 8 and 17 Sep, reaching a maximum of 0.99 mg m^{-3} on 19 Sep. The initial increase is attributed to upward Chla entrainment, whereas the delayed increase is attributed to new production from ventilation of the nutricline. Based on these measurements we estimate that new production contributed about 70% to the total. By 27–28 Sep, Chla had decreased from 0.81 to 0.45 mg m^{-3} in the northern feature and from 0.99 to 0.24 mg m^{-3} in the southern feature (Table 2). Both blooms experienced horizontal entrainment around the WCR and mixing with adjacent waters due to strong currents (60–80 cm s^{-1}) (Figure 3c). The Chla response in GoM cyclones was larger than previous observations in the oligotrophic Atlantic [*Babin et al.*, 2004].

[12] On 19 Sep, a 200-km long filament of pigment-rich shelf and river water was detected in Chla imagery, extending SE from the Mississippi River delta along the north flank of the WCR (Figure 3c). Seaward entrainment of this coastal water mass was confirmed by NDBC buoy 42040, which broke free from its mooring and moved seaward at a mean speed of 66 cm s^{-1} from 17–20 Sep (Figure 3c). The buoy moved within relatively clear water, which separated the shelf filament from the plankton bloom within the cyclone (Figure 3c). The satellite-derived Chla estimates within the shelf filament (1–5 mg m^{-3}) may be overestimates of in-situ values due to high levels of river-borne suspended sediment and/or CDOM. Similar pigment-rich coastal filaments have been observed after hurricanes along the NE U.S. coast [*Davis and Yan*, 2004] and in the northern GoM [*Yuan et al.*, 2004]. Their importance in delivering carbon to deeper oligotrophic regions has been discussed [*Yuan et al.*, 2004].

4. Summary and Conclusions

[13] Satellite-derived SST, SSH, and Chla measurements clearly revealed rapid upwelling responses along and east of Ivan's path where pre-existing cyclonic circulation experienced intensification. Venting of thermoclines and nutriclines can explain the SST cooling response of 3–7°C and subsequent Chla enhancement. Although hurricane-forced SST change and augmentation in Chla have been reported in the Atlantic Ocean, an association with cold-core cyclones has not previously been made. Our results support the contention that wind-enhanced eddy pumping of nutrients into surface waters is an important process in biogeochemical cycling as discussed by *McGillicuddy et al.* [1998] and *Falkowski et al.* [1991]. Recent improvements in the repeat coverage from satellite altimeters will enhance capabilities for detecting cold-core cyclones, which can not easily be detected in satellite SST data until a wind event initiates upwelling and, in extreme cases such as this one, surface cooling.

[14] We observed evidence of rapid negative ocean-atmosphere feedback to Hurricane Ivan from the large areas of cooling where SSTs of 20–26°C were generated during hurricane passage. Thus, mesoscale ocean cyclones, in addition to warm anticyclones, may play an important role in along track hurricane intensity changes. We suggest that hurricane intensity forecasts may benefit from the inclusion of more accurate location and intensity information on oceanic cyclones. This could be accomplished by including an eddy-resolving data assimilative ocean modeling capability in coupled atmosphere/ocean hurricane simulations.

[15] **Acknowledgments.** This research was funded by the Minerals Management Service – LSU Coastal Marine Institute Cooperative Agreement 1435-01-99-CA-30951/85247 and the LA Board of Regents Millenium Trust Health Excellence Fund, Contract HEF (2001-06) -01. Adele Babin, Alaric Haag, Jessica Crochet, and Chet Pilley are thanked for data processing assistance; Clifford Duplechin for computer graphics.

References

Babin, S. M., J. A. Carton, T. D. Dickey, and J. D. Wiggert (2004), Satellite evidence of hurricane-induced phytoplankton blooms in an oceanic desert, *J. Geophys. Res.*, *109*, C03043, doi:10.1029/2003JC001938.

Biggs, D. C., and F. E. Muller-Karger (1994), Ship and satellite observations of chlorophyll stocks in interacting cyclone-anticyclone eddy pairs in the western Gulf of Mexico, *J. Geophys. Res.*, *99*, 7371–7384.

Black, P. G., and G. J. Holland (1995), The boundary layer of tropical Cyclone Kerry (1979), *Mon. Weather Rev.*, *123*, 2007–2028.

Brand, S. (1971), The effects on a tropical cyclone of cooler surface waters due to upwelling and mixing produced by a prior tropical cyclone, *J. Appl. Meteorol.*, *10*, 865–874.

Buyers, H. R. (1974), *General Meteorology*, 314 pp., McGraw-Hill, New York.

Davis, A., and X. Yan (2004), Hurricane forcing on chlorophyll-a concentration off the northeast coast of the U.S., *Geophys. Res. Lett.*, *31*, L17304, doi:10.1029/2004GL020668.

Emanuel, K. A. (1999), Thermodynamic control of hurricane intensity, *Nature*, *401*, 665–669.

Falkowski, P. G., D. Ziemann, Z. Kolber, and P. K. Bienfang (1991), Role of eddy pumping in enhancing primary production in the ocean, *Nature*, *352*, 55–58.

Gilligan, M. J., and J. Blaha (2003), Gulf of Mexico Airborne Survey, January 2000: Dynamic height determination using airborne expendable bathythermographs, *Tech. Note TN 01-03*, Naval Oceanographic Office, Stennis Space Center, Miss.

Leben, R. R., G. H. Born, and B. R. Engebreth (2002), Operational altimeter data processing for mesoscale monitoring, *Mar. Geod.*, *25*, 3–18.

Legeckis, R., P. C. T. Zhu, and S. Chen (1999), Satellite animations reveal ocean surface dynamics for shortest timescales ever, *EOS Trans. AGU*, *80*(20), 229, 232–233.

McGillicuddy, D. J., A. R. Robinson, D. A. Siegel, H. W. Jannasch, R. Johnson, T. D. Dickey, J. McNeil, A. F. Michaels, and A. H. Knap (1998), Influence of mesoscale eddies on new production in the Sargasso Sea, *Nature*, *394*, 263–266.

Monaldo, F. M., T. D. Sikora, S. M. Babin, and R. E. Sterner (1997), Satellite imagery of sea surface temperature cooling in the wake of Hurricane Edouard, (1996), *Mon. Weather Rev.*, *125*, 2716–2721.

National Hurricane Center (2004), Tropical cyclone report: Hurricane Ivan, Natl. Weather Serv., Silver Spring, Md. (Available at http://www.nws.noaa.gov)

O'Reilly, J. E., S. Maritorena, B. G. Mitchell, D. Siegel, K. Carder, S. Garver, M. Kahru, and C. McClain (1998), Ocean color chlorophyll algorithms for SeaWiFS, *J. Geophys. Res.*, *103*, 24,937–24,953.

Price, J. F. (1981), Upper ocean response to a hurricane, *J. Phys. Oceanogr.*, *11*, 153–175.

Price, J. F., T. B. Sanford, and G. Z. Forristall (1994), Forced stage response to a moving hurricane, *J. Phys. Oceanogr.*, *24*, 233–260.

Sanford, T. B., P. G. Black, J. R. Haustein, J. W. Feeney, G. Z. Forristall, and J. F. Price (1987), Ocean response to a hurricane, Part I: observations, *J. Phys. Oceanogr.*, *17*, 2065–2083.

Shay, L. K., G. J. Goni, and P. G. Black (2000), Effects of a warm oceanic feature on Hurricane Opal, *Mon Weather Rev.*, *128*, 1366–1383.

Stramma, L., P. Cornillon, and J. F. Price (1986), Satellite observations of sea surface cooling by hurricanes, *J. Geophys. Res.*, *91*, 5031–5035.

Walker, N., S. Myint, A. Babin, and A. J. Haag (2003), Advances in satellite radiometry for the surveillance of surface temperatures, ocean eddies and upwelling processes in the Gulf of Mexico using GOES-8 measurements during summer, *Geophys. Res. Lett.*, *30*(16), 1854, doi:10.1029/2003GL017555.

Yuan, J., R. L. Miller, R. T. Powell, and M. J. Dagg (2004), Storm-induced injection of the Mississippi River plume into the open Gulf of Mexico, *Geophys. Res. Lett.*, *31*, L09312, doi:10.1029/2003GL019335.

Zimmerman, R. A., and D. C. Biggs (1999), Patterns of distribution of sound-scattering zooplankton in warm- and cold-core eddies in the Gulf of Mexico, from a narrowband acoustic Doppler current profiler survey, *J. Geophys. Res.*, *104*, 5251–5262.

S. Balasubramanian, Coastal Studies Institute Earth Scan Laboratory, Louisiana State University, Baton Rouge, LA 70803, USA.

R. R. Leben, Colorado Center for Astrodynamics Research, University of Colorado, Boulder, CO USA.

N. D. Walker, Department of Oceanography and Coastal Sciences/ Coastal Studies Institute Earth Scan Laboratory, Louisiana State University, Baton Rouge, LA 70803, USA. (nwalker@lsu.edu)